Electronic Supplementary Material (ESI) for Nanoscale.

Supplementary Information

In-situ cathodic activation of V-incorporated Ni_xS_y nanowires for enhanced hydrogen evolution

Xiao Shang [a], Kai-Li Yan [a], Yi Rao [a, b], Bin Dong [*a, b], Jing-Qi Chi [a], Yan-Ru Liu [a], Xiao Li [a], Yong-Ming Chai [a], Chen-Guang Liu [*a]

a State Key Laboratory of Heavy Oil Processing, China University of Petroleum (East China), Qingdao 266580, PR China

b College of Science, China University of Petroleum (East China), Qingdao 266580, PR China

∗ Corresponding author. Email: dongbin@upc.edu.cn (B. Dong), cgliu@upc.edu.cn(C.-G. Liu)

Tel: +86-532-86981376, Fax: +86-532-86981787

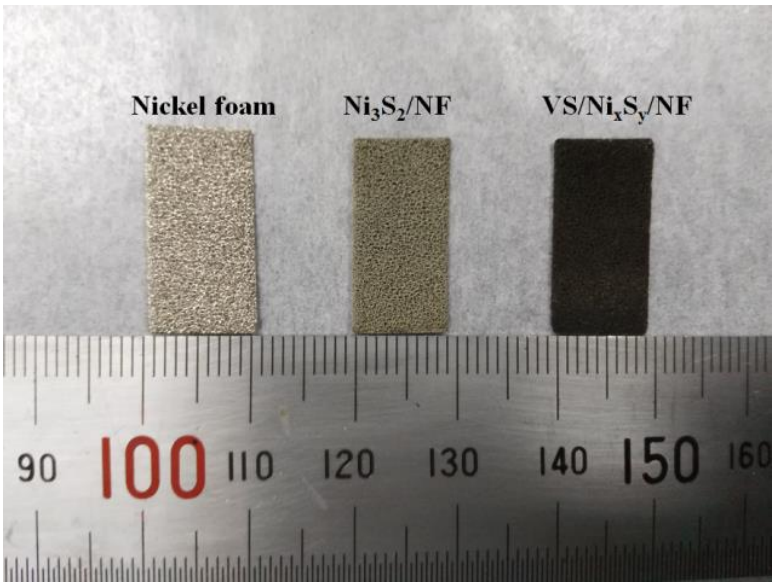

Figure S1. Photographs of the as-prepared samples.

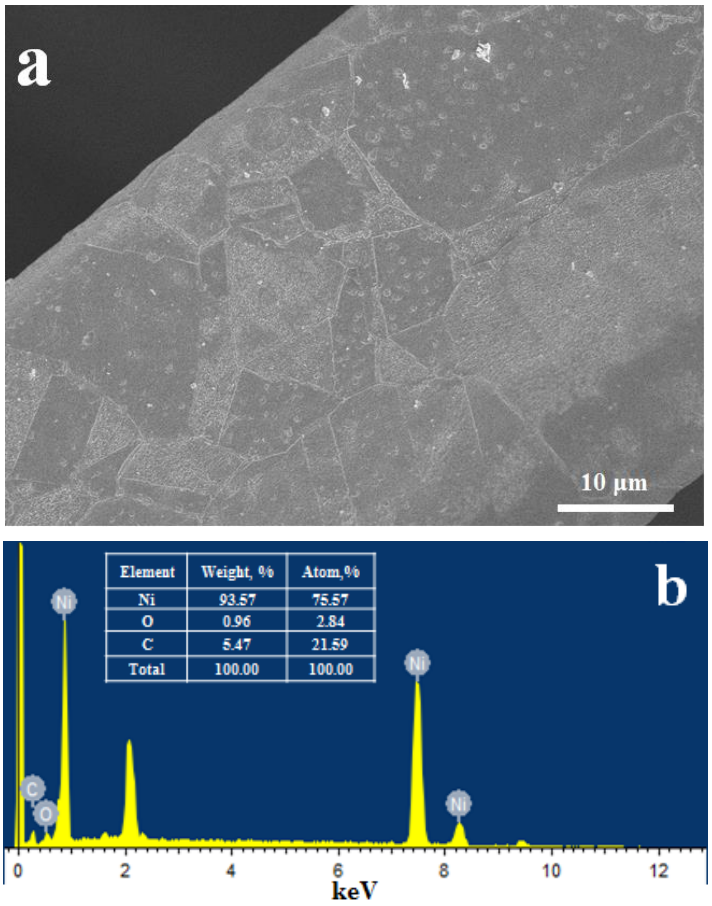

Figure S2. (a) SEM image of bare nickel foam (NF). (b) X-ray fluorescence elemental analysis (EDX) spectra of NF.

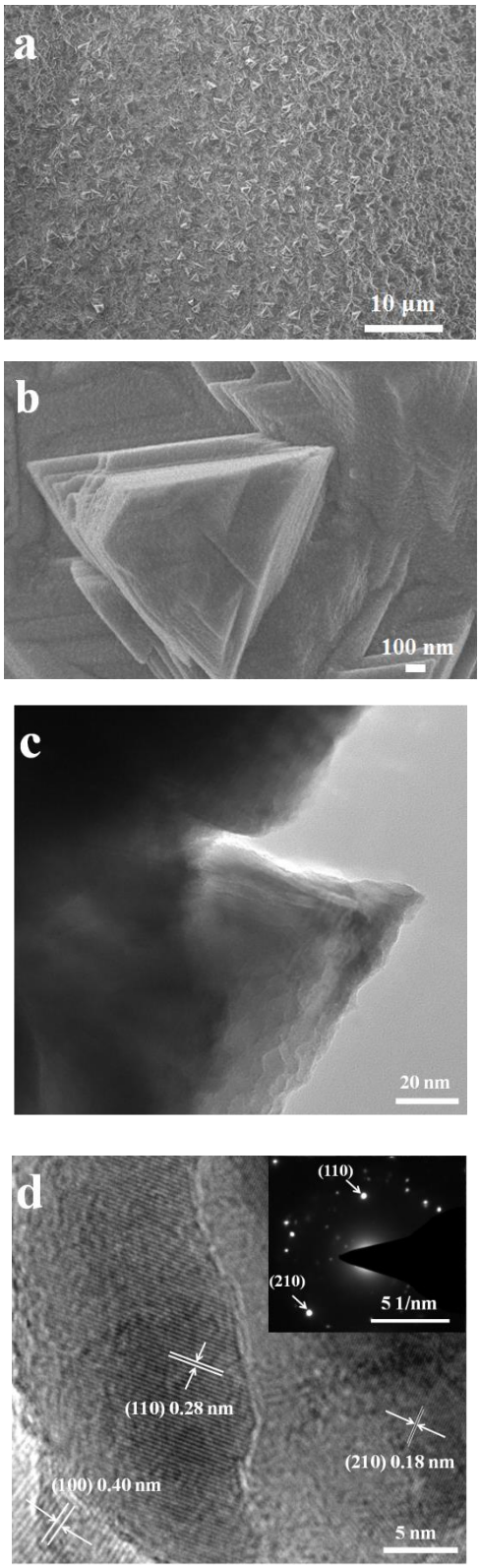

Figure S3. (a, b) SEM images of Ni_3S_2/NF. (c) TEM and (d) high-resolution transmission electron microscopy (HRTEM) of Ni_3S_2/NF (insertion: selected area electron diffraction (SAED) of Ni_3S_2/NF).

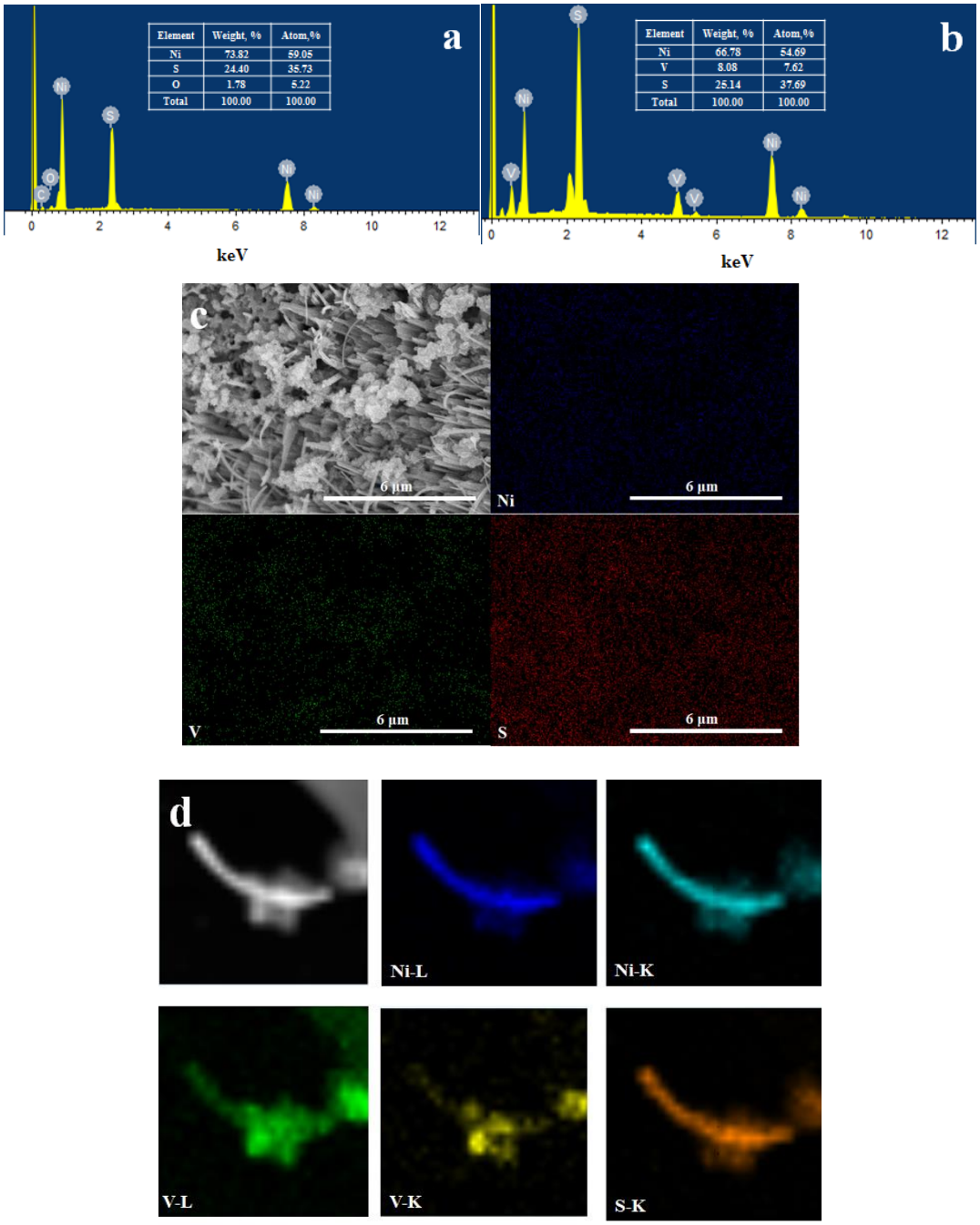

Figure S4. EDX spectra of (a) Ni_3S_2/NF and (b) VS/Ni_xS_y/NF. (c) SEM mapping of VS/Ni_xS_y/NF. (d) TEM mapping of VS/Ni_xS_y nanowire on VS/Ni_xS_y/NF.

Calculation method of electrochemically active surface area (ECSA)

According to previous report,[1] the calculation of ECSA and roughness factor (RF) are based on the following equations:

$$ECSA=C_{dl}/Cs \quad (1)$$

$$RF=ECSA/GSA \quad (2)$$

In eq (1), C_{dl} is the measured double layer capacitance of samples in 1.0 M KOH (mF) and C_s is the specific capacitance of the catalyst (C_s = 0.04 mF cm^{-2} in 1.0 M KOH). In eq (2), RF is roughness factor and GSA is geometric surface area of the samples (2.00 cm^2).

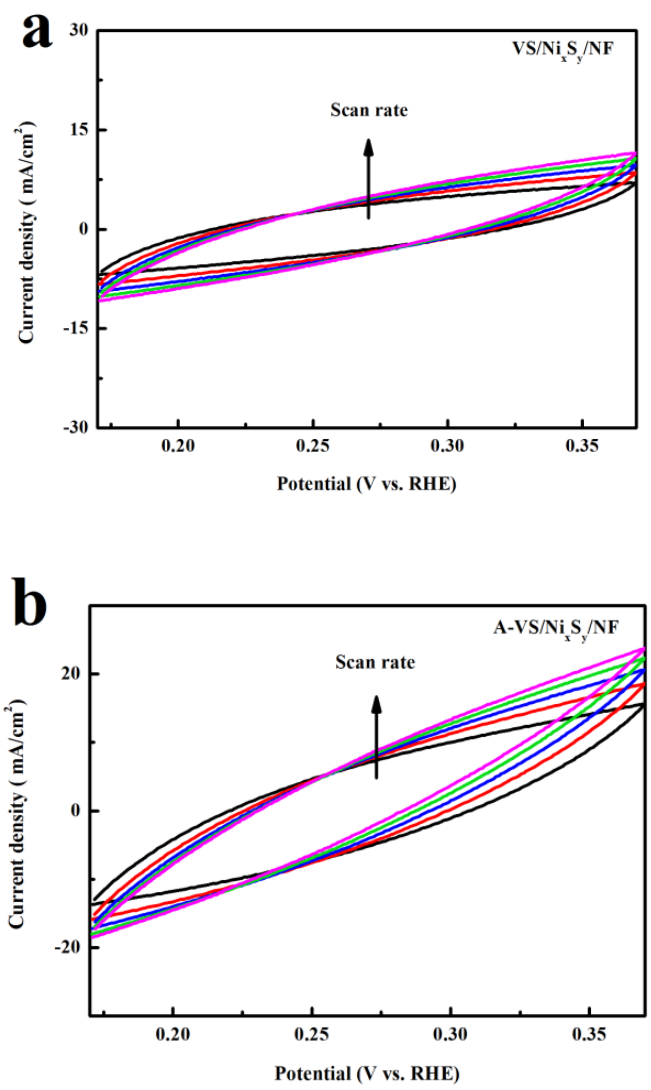

Figure S5. Cyclic voltammogram (CV) of double-layer capacitance measurement of (a) VS/Ni_xS_y/NF and (b) A-VS/Ni_xS_y/NF.

Table S1. The calculated ECSA and RF of all samples.

Sample	C_{dl}, mF	Cs, mF cm^{-2}	ECSA, $\times 10^3$ cm^2	GSA, cm^2	RF $\times 10^3$
VS/Ni_xS_y/NF	44.46	0.04	1.11	2.00	0.56
A-VS/Ni_xS_y/NF	82.92	0.04	2.07	2.00	1.04

Table S2. Elemental values of fitted equivalent circuit of $VS/Ni_xS_y/NF$ and $A\text{-}VS/Ni_xS_y/NF$.

Samples	R_s/Ω	R_{ct}/Ω
$VS/Ni_xS_y/NF$	1.5	952.0
$A\text{-}VS/Ni_xS_y/NF$	1.0	13.0

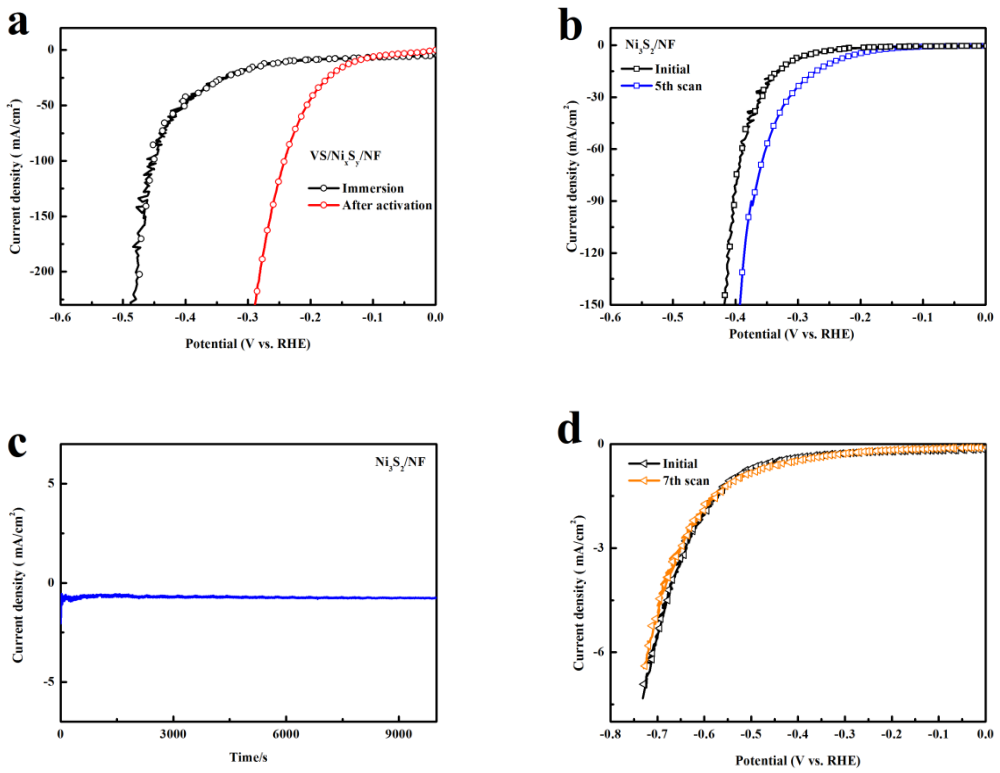

Figure S6. (a) In-situ cathodic activation (ISCA) of (a) I-VS/Ni_xS_y/NF and (b) Ni_3S_2/NF. (c) Chronoamperometry of Ni_3S_2/NF for 10^4 s. (d) ISCA of VS powder.

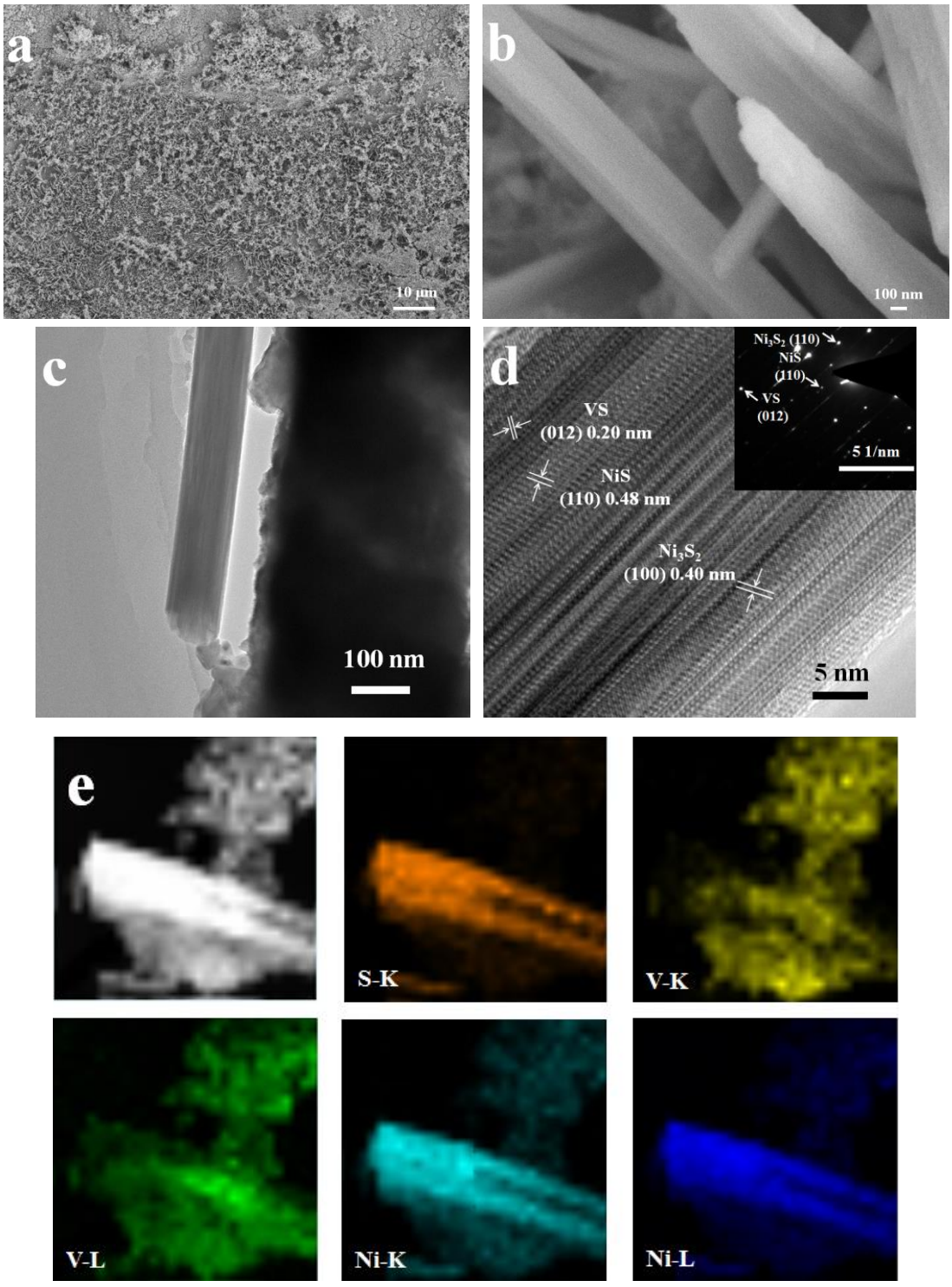

Figure S7. (a, b) SEM images of I-VS/Ni_xS_y/NF. (c) TEM and (d) HRTEM of I-VS/Ni_xS_y/NF (insertion: SAED of I-VS/Ni_xS_y/NF). (e) TEM mapping of VS/Ni_xS_y nanowire on I-VS/Ni_xS_y/NF.

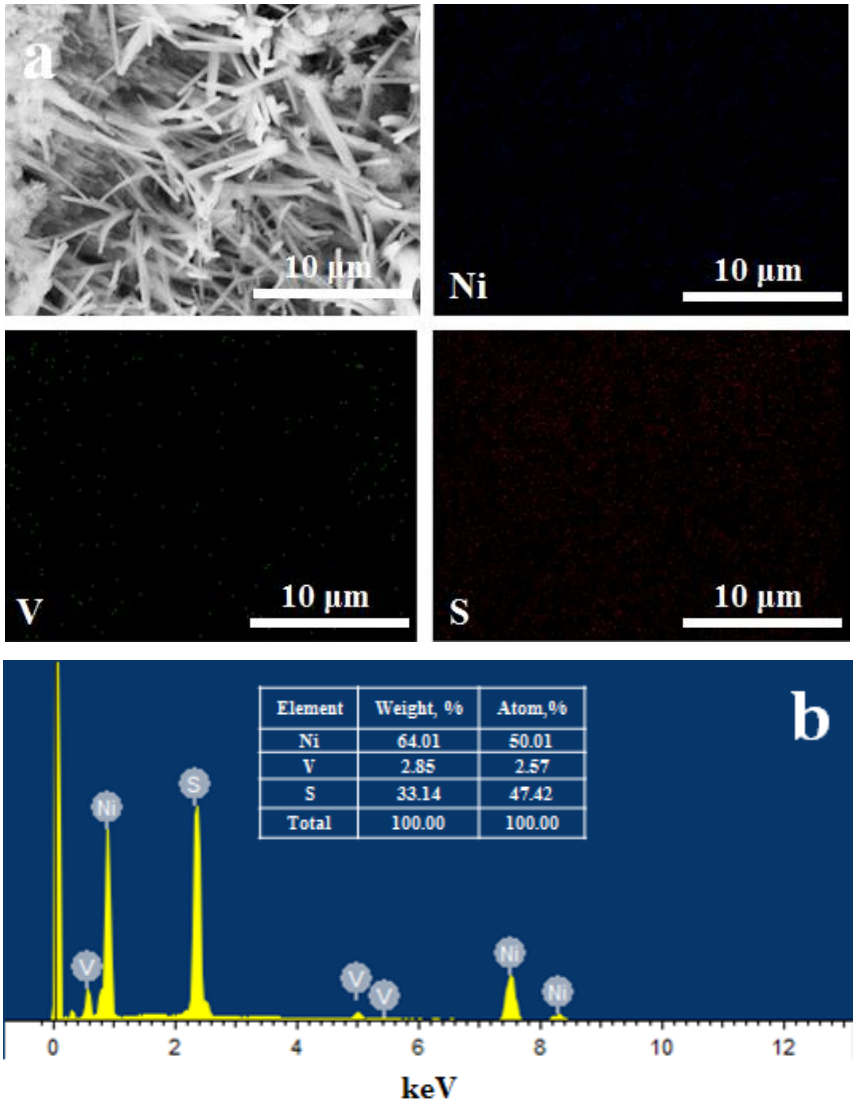

Figure S8. (a) SEM mapping and (b) EDX spectrum of I-VS/Ni_xS_y/NF.

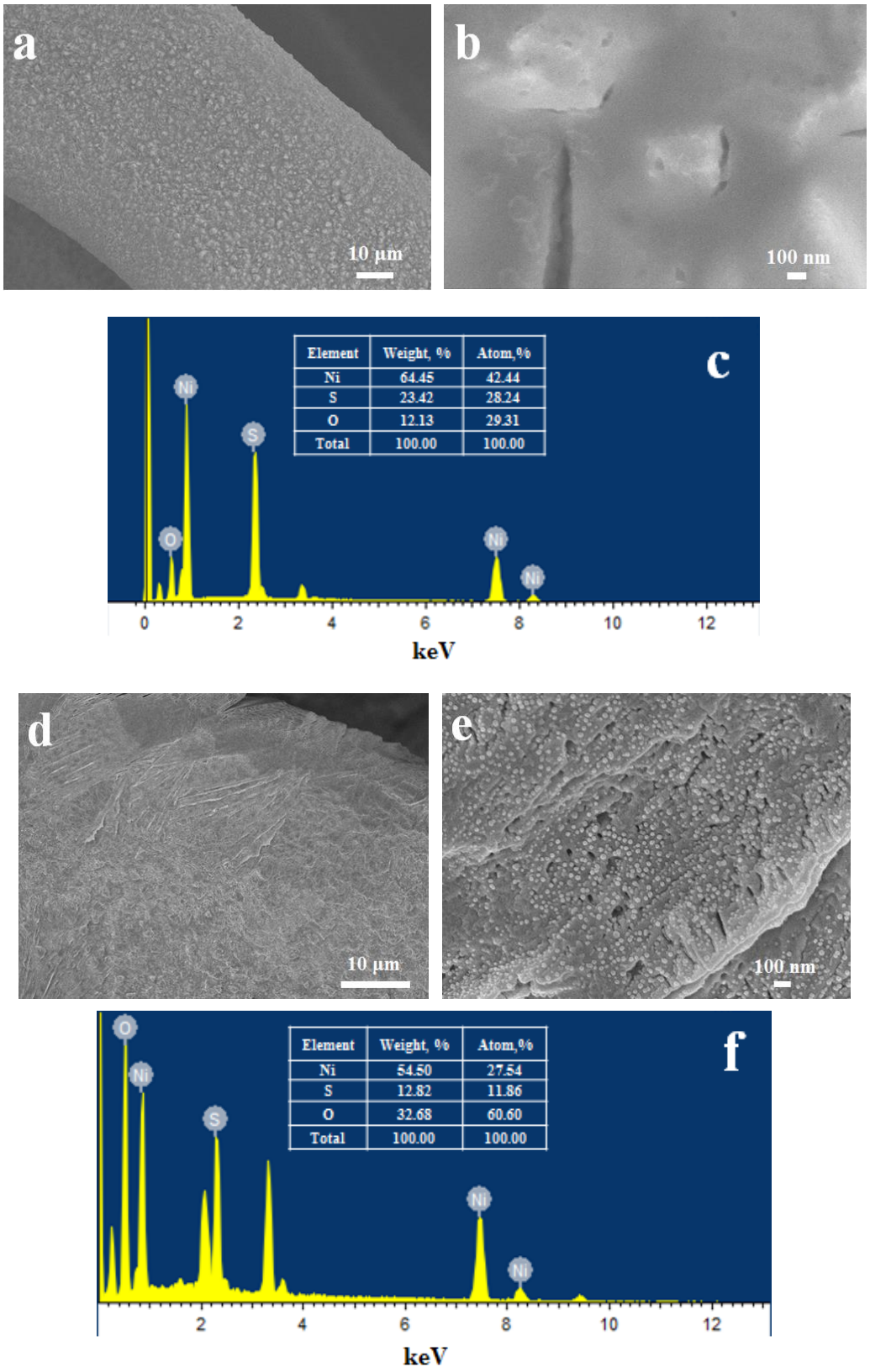

Figure S9. (a, b) SEM images and (c) EDX spectrum of Ni_3S_2/NF after ISCA. (d, e) SEM images and (f) EDX spectrum of Ni_3S_2/NF after chronoamperometry for 10^4 s.

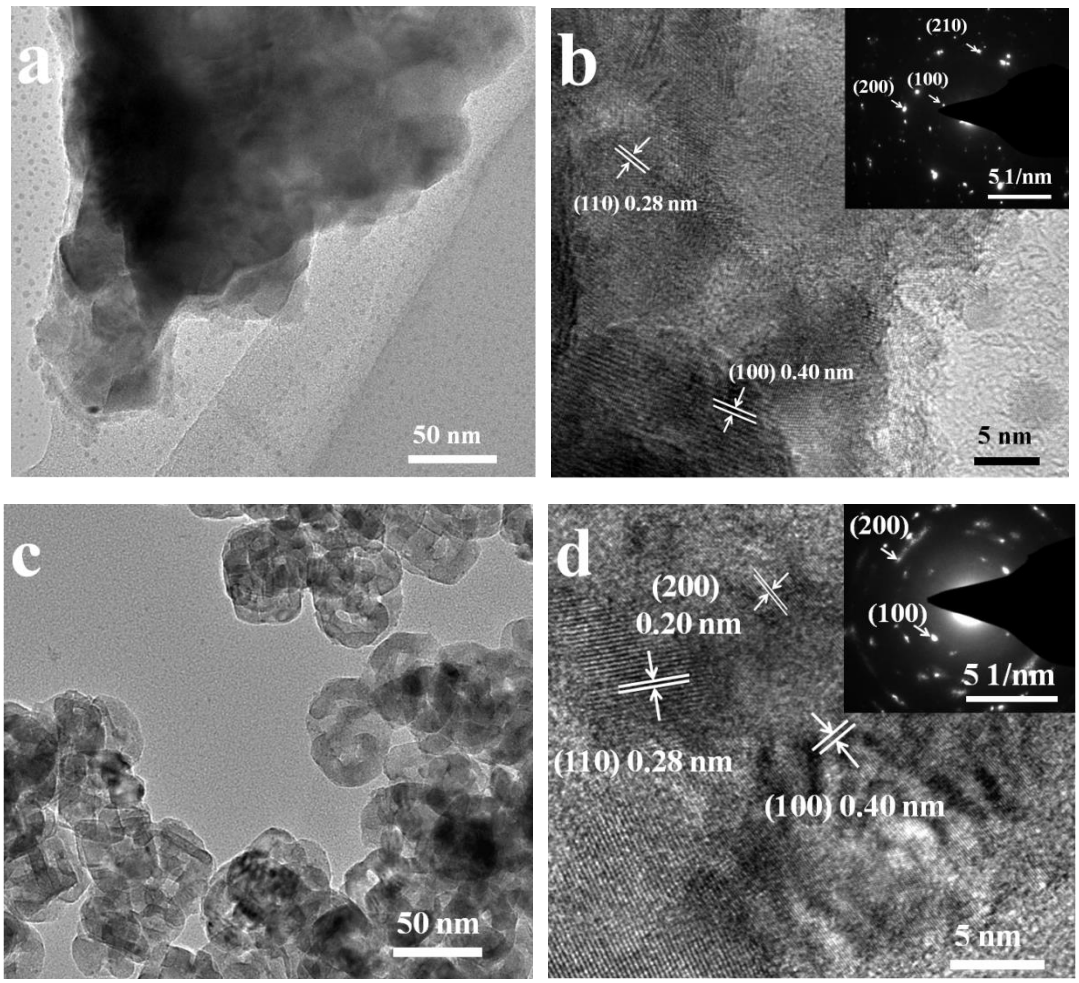

Figure S10. (a) TEM and (b) HRTEM of Ni_3S_2/NF after ISCA (insertion: SAED of Ni_3S_2/NF after LSV). (c) TEM and (d) HRTEM of Ni_3S_2/NF after chronoamperometry for 10^4 s at an overpotential of 130 mV (insertion: the corresponding SAED).

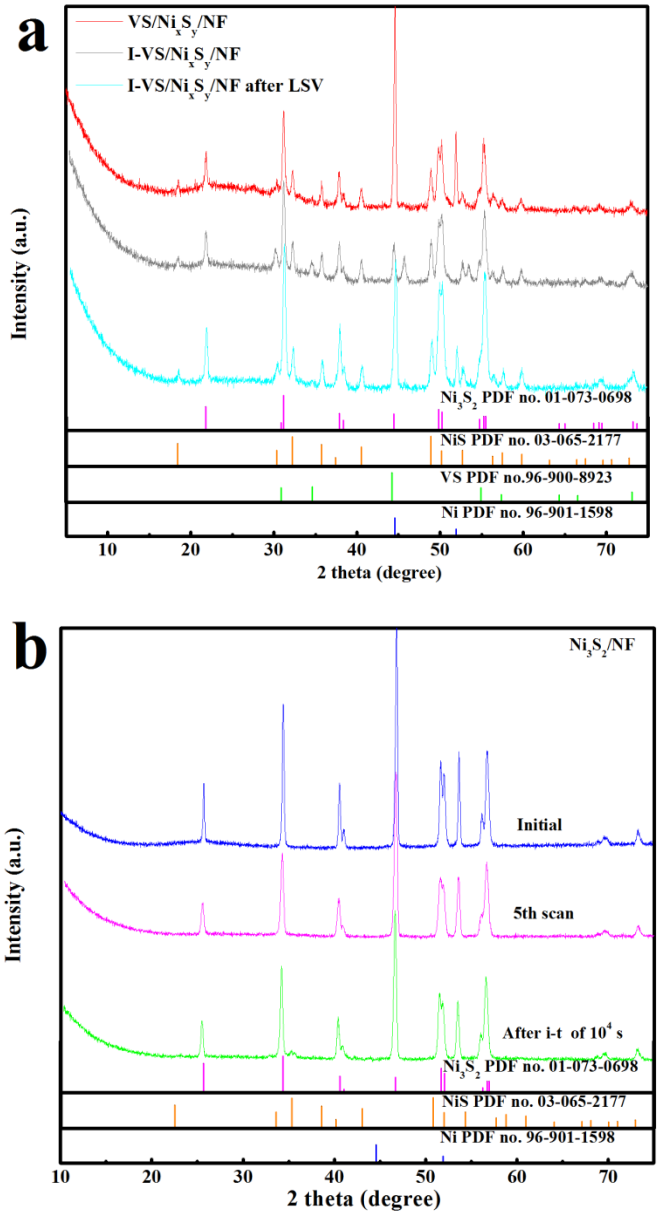

Figure S11. XRD patterns. (a) VS/Ni_xS_y/NF, I-VS/Ni_xS_y/NF and I-VS/Ni_xS_y/NF after ISCA. (b) Ni_3S_2/NF, Ni_3S_2/NF after LSV and Ni_3S_2/NF after chronoamperometry for 10^4 s at an overpotential of 130 mV.

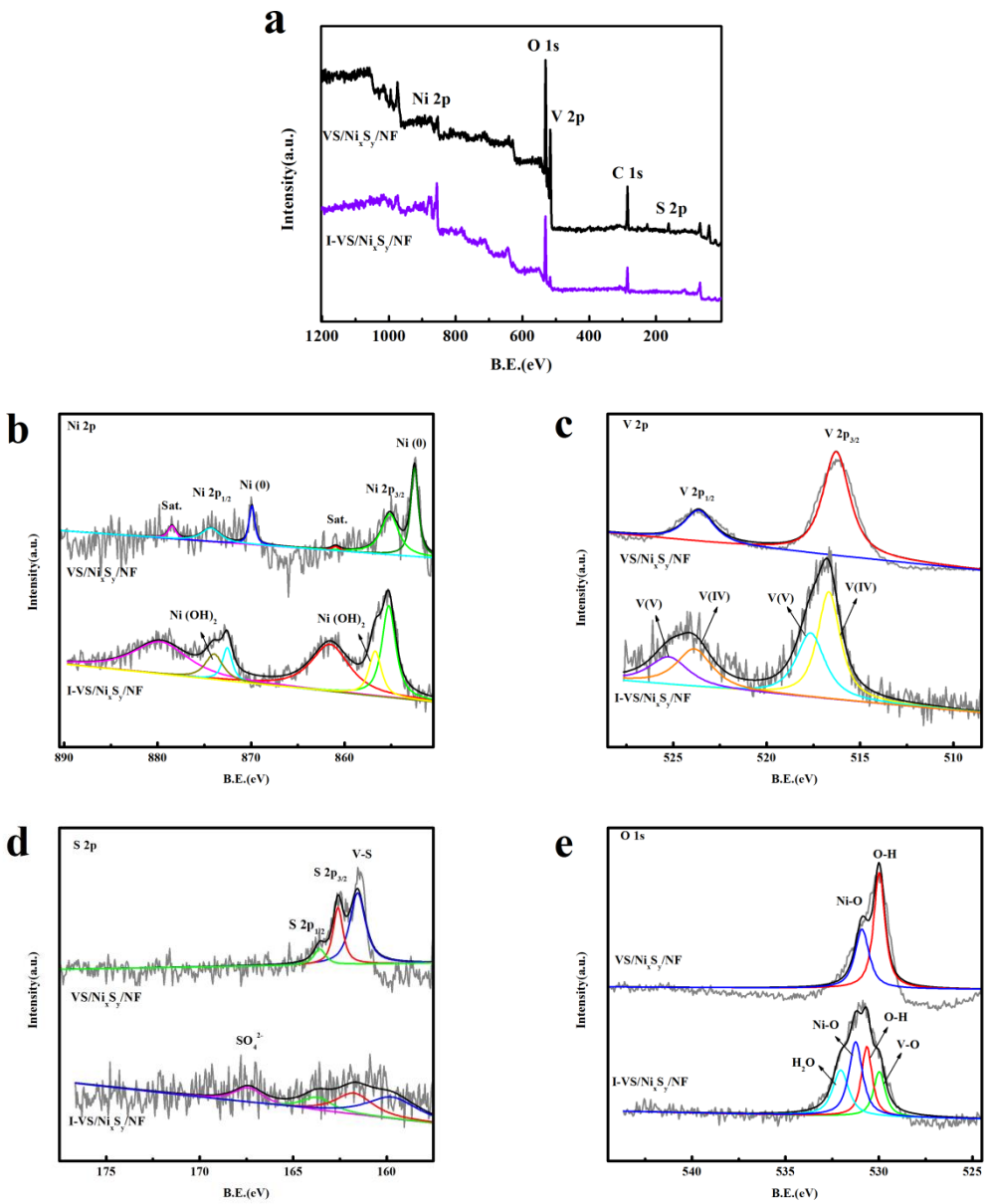

Figure S12. XPS spectra of I-VS/Ni$_x$S$_y$/NF. (a) Survey. (b) Ni 2p. (c) V 2p. (d) S 2p. (e) O 1s.

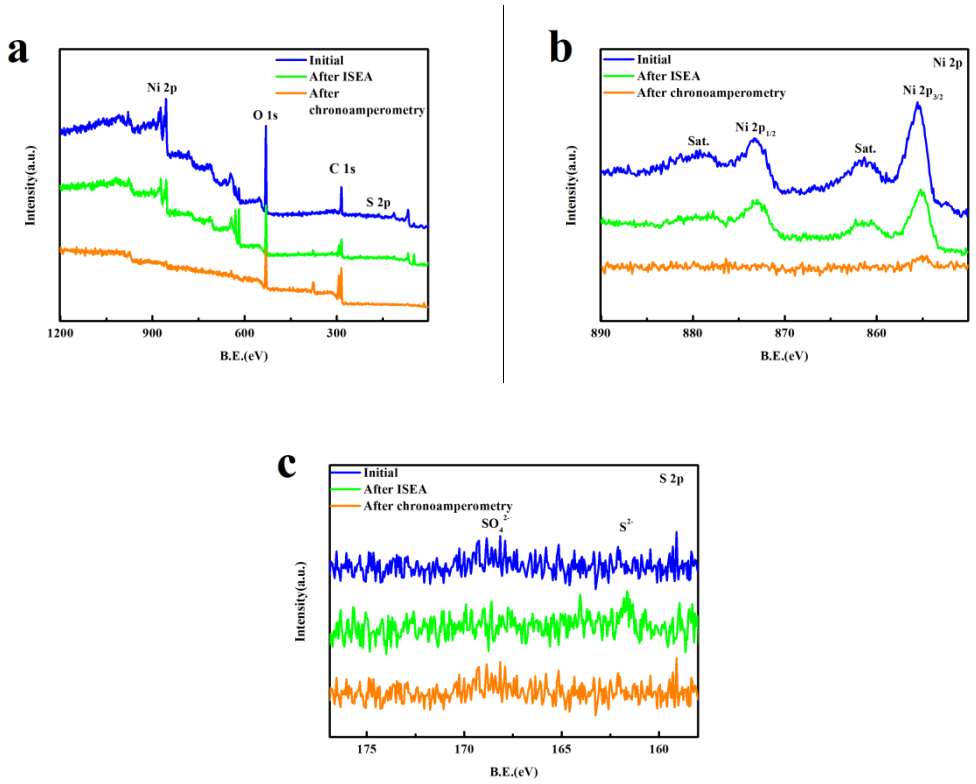

Figure S13. XPS spectra of Ni_3S_2/NF, Ni_3S_2/NF after ISCA and Ni_3S_2/NF after chronoamperometry for 10^4 s at an overpotential of 130 mV. (a) Survey. (b) Ni 2p. (c) S 2p.

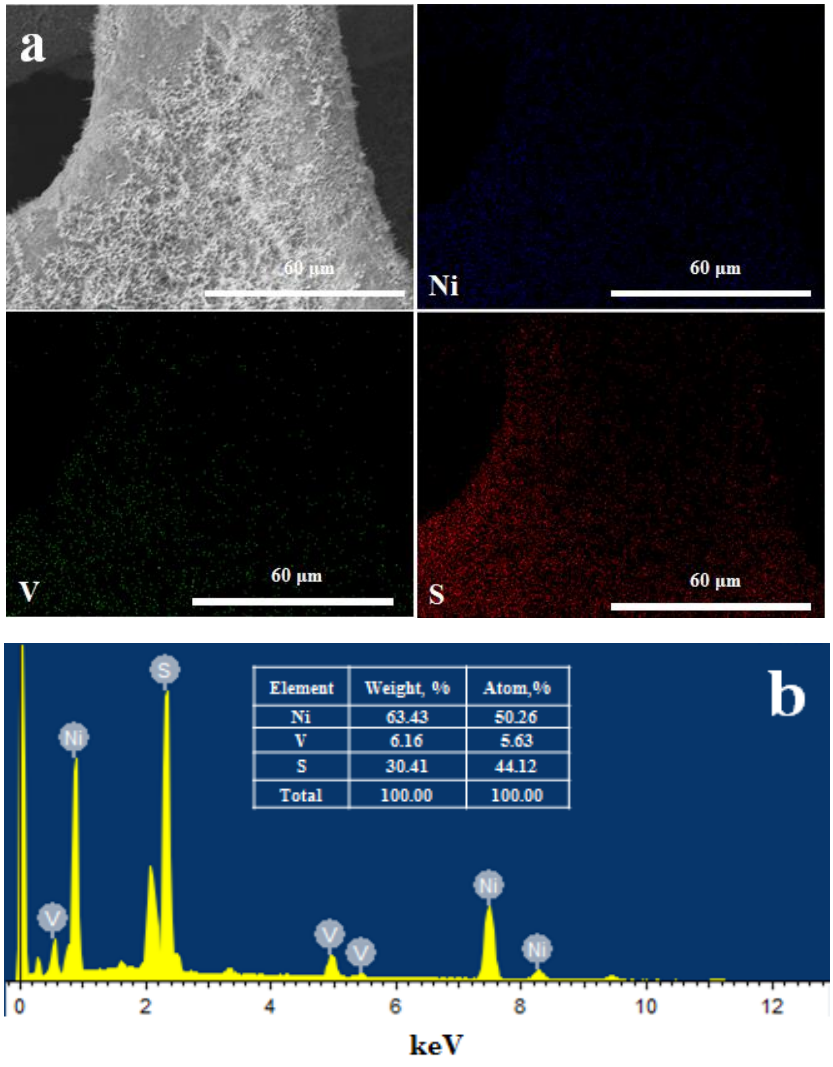

Figure S14. (a) SEM mapping and (b) EDX of A-VS/Ni_xS_y/NF.

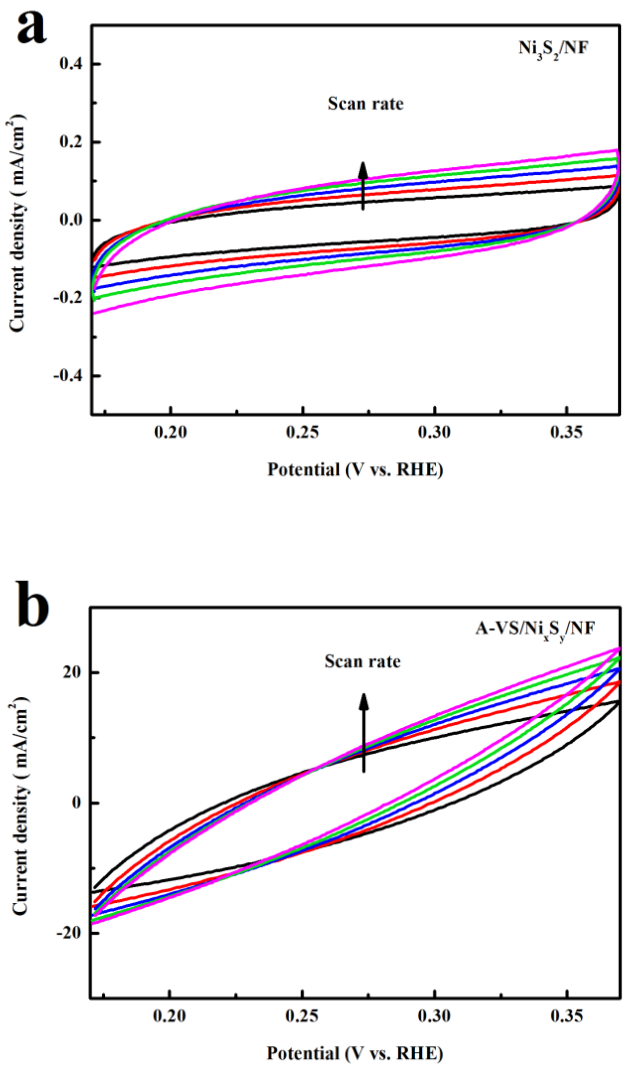

Figure S15. CVs of double-layer capacitance measurement of (a) Ni_3S_2/NF and (b) A-VS/Ni_xS_y/NF.

Table S3. Elemental values of fitted equivalent circuit of NF, Ni_3S_2/NF and A-VS/Ni_xS_y/NF.

Samples	R_s/Ω	R_{ct}/Ω
NF	1.5	69
Ni_3S_2/NF	1.3	31.3
A-VS/Ni_xS_y/NF	1.0	13.0

Table S4. The calculated ECSA and RF of all samples.

Sample	C_{dl}, mF	Cs, mF cm^{-2}	ECSA, $\times 10^3$ cm^2	GSA, cm^2	RF $\times 10^3$
Ni_3S_2/NF	3.04	0.04	0.08	2.00	0.04
A-VS/Ni_xS_y/NF	82.92	0.04	2.07	2.00	1.04

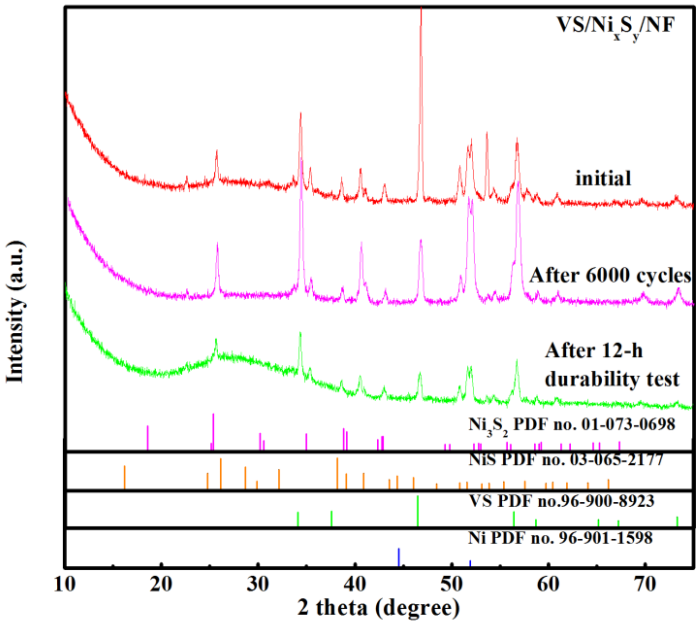

Figure S16. XRD patterns of initial $VS/Ni_xS_y/NF$ before and after stability test.

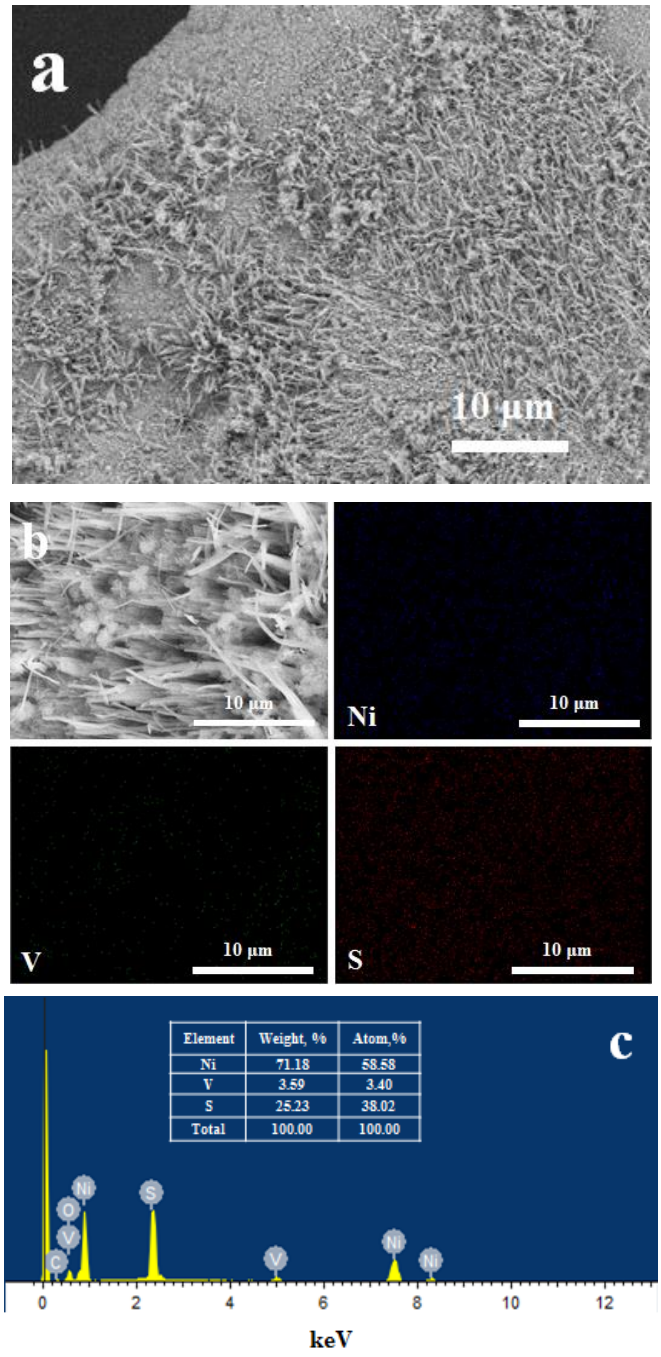

Figure S17. (a) SEM image, (b) SEM mapping and (c) EDX of A-VS/Ni_xS_y/NF after stability test of CV.

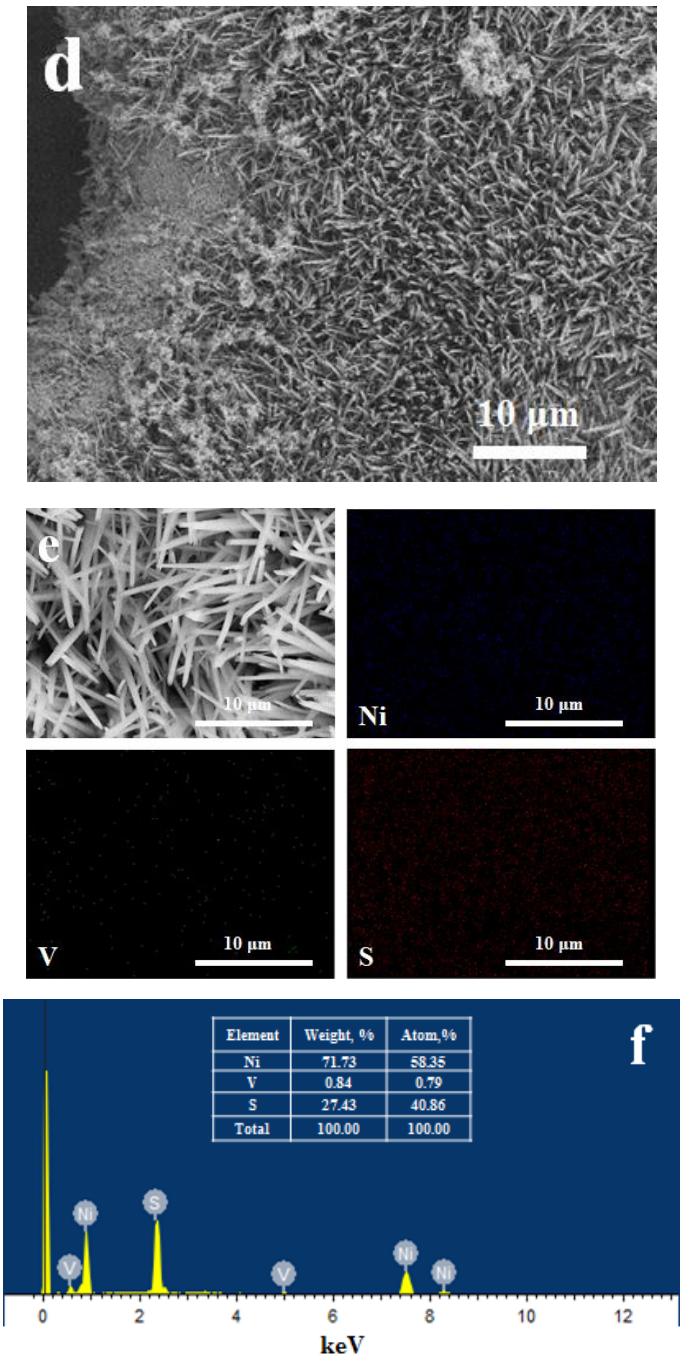

Figure S17. (d) SEM image, (e) SEM mapping and (f) EDX of A-VS/Ni_xS_y/NF after stability test of chronoamperometry for 12 h at an overpotential of 130 mV.

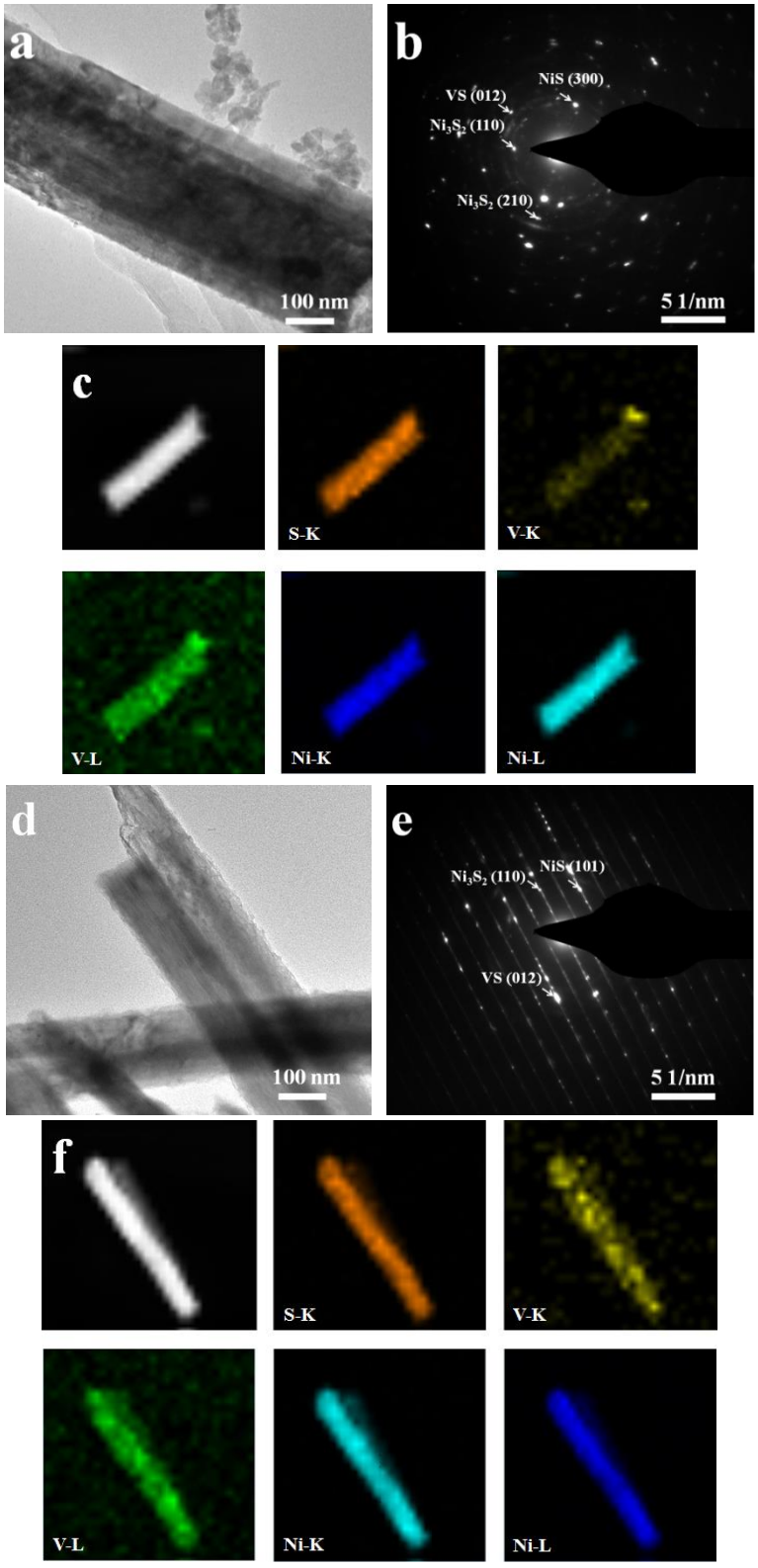

Figure S18. (a) TEM, (b) HRTEM and (c) TEM mapping of A-VS/Ni_xS_y/NF after stability test of CV. (c) TEM , (d) HRTEM and (e) TEM mapping of A-VS/Ni_xS_y/NF after stability test of chronoamperometry for 12 h at an overpotential of 130 mV.

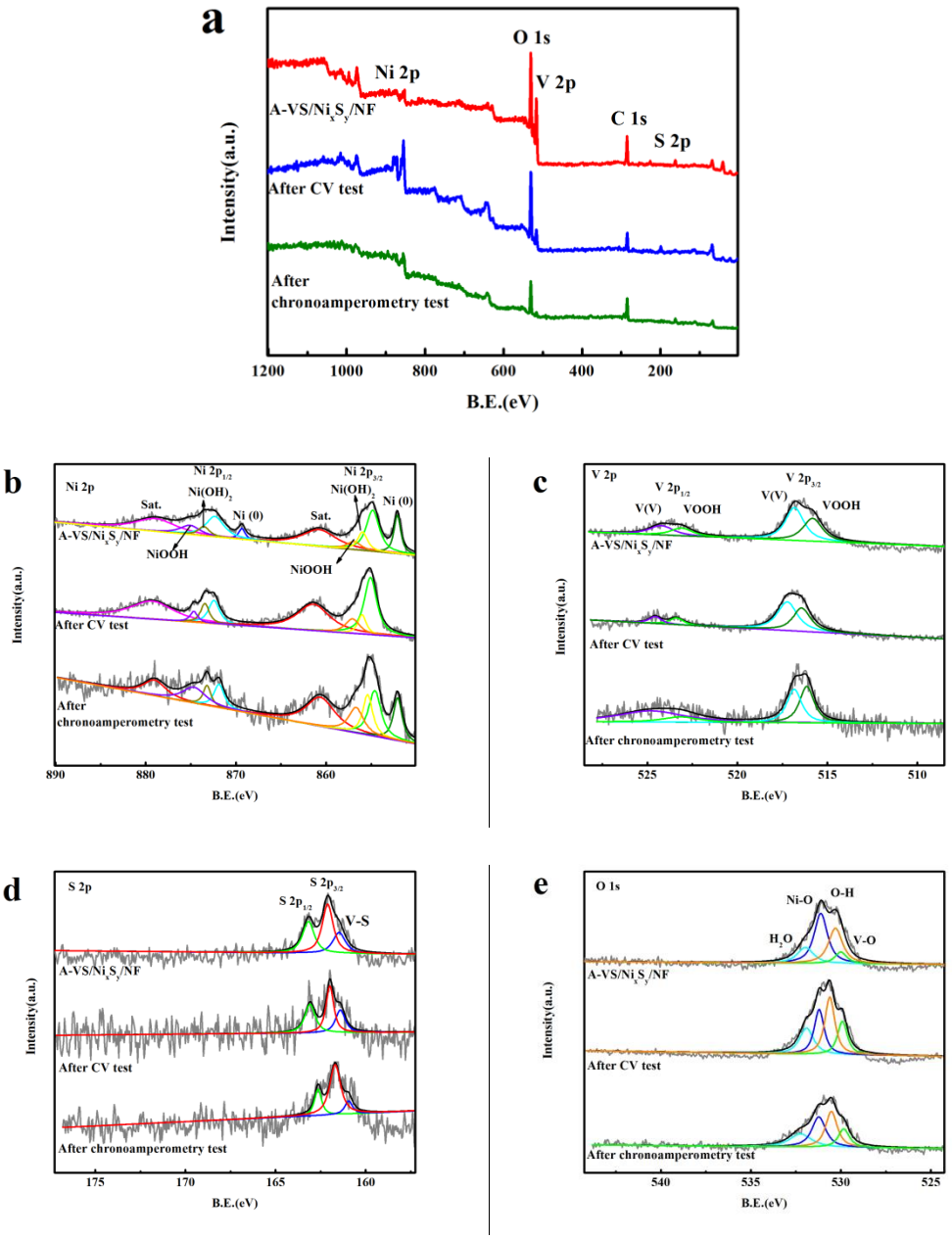

Figure S19. XPS spectra of A-VS/Ni_xS_y/NF after stability test. (a) Survey. (b) Ni 2p. (c) V 2p. (d) S 2p. (e) O 1s.

Table S5. Comparison of alkaline HER activities of nickel sulfide-based materials.

Sample	Electrolyte	Current density j mA cm-2	Overpotential η at corresponding j (mV)	Tafel slope (mV dec^{-1})	Ref.
Ni-Mn_3O_4	1.0 M KOH	10	91	110	[2]
NiS_2-MoS_2	1.0 M KOH	400	400	70	[3]
MoS_2/Ni_3S_2	1.0 M KOH	10	110	83	[4]
MoO_x/Ni_3S_2/NF	1.0 M KOH	ca.500	<500	90	[5]
High-index faceted Ni_3S_2	1.0 M KOH	10	223	—	[6]
Mo-doped Ni_3S_2	1.0 M KOH	100	278	72.9	[7]
$NiCo_2S_4$/carbon cloth	1.0 M KOH	100	305	141	[8]
$NiCo_2S_4$/Ni foam	1.0 M KOH	10	65	84.5	[9]
NiFeS/NF	1.0 M KOH	10	180	53	[10]
rGO/$(Ni_xMn_yCo_z)_3S_4$	1.0 M KOH	10	151	52	[11]
Co_9S_8-Ni_xS_y/Ni foam	1.0 M KOH	10	163	88	[12]
VS/Ni_xS_y/Ni foam	1.0 M KOH	10	125	113	This work

References

1 C. C. McCrory, S. Jung, J. C. Peters and T. F. Jaramillo, *J. Am. Chem. Soc.*, 2013, **135**, 16977-16987.

2 X. Li, P. F. Liu, L. Zhang, M. Y. Zu, Y. X. Yang and H. G. Yang, *Chem.Commun.*, 2016, **52**, 10566-10569.

3 T. An, Y. Wang, J. Tang, W. Wei, X. Cui, A. M. Alenizi, L. Zhang and G. Zheng, *J.Mater. Chem. A*, 2016, **4**, 13439-13443.

4 J. Zhang, T. Wang, D. Pohl, B. Rellinghaus, R. Dong, S. Liu, X. Zhuang and X. Feng, *Angew. Chem. Int. Ed.*, 2016, **128**, 6814-6819.

5 Y. Wu, G. D. Li, Y. Liu, L. Yang, X. Lian, T. Asefa and X. Zou, *Adv. Funct. Mater.*, 2016, **26**, 4839-4847.

6 L.-L. Feng, G. Yu, Y. Wu, G.-D. Li, H. Li, Y. Sun, T. Asefa, W. Chen and X. Zou, *J. Am. Chem. Soc*, 2015, **137**, 14023-14026.

7 Z. Cui, Y. Ge, H. Chu, R. Baines, P. Dong, J. Tang, Y. Yang, P. M. Ajayan, M. Ye and J. Shen, *Journal of Materials Chemistry A*, 2017, DOI: 10.1039/C6TA09853C.

8 D. Liu, Q. Lu, Y. Luo, X. Sun and A. M. Asiri, *Nanoscale*, 2015, **7**, 15122-15126.

9 L. Ma, Y. Hu, R. Chen, G. Zhu, T. Chen, H. Lv, Y. Wang, J. Liang, H. Liu and C. Yan, *Nano Energy*, 2016, **24**, 139-147.

10 P. Ganesan, A. Sivanantham and S. Shanmugam, *J. Mater. Chem. A*, 2016, **4**, 16394-16402.

11 R. Miao, J. He, S. Sahoo, Z. Luo, W. Zhong, S.-Y. Chen, C. Guild, T. Jafari, B. Dutta and S. A. Cetegen, *ACS Catal.*, 2016, **7** , 819-832.

12 D. Ansovini, C. J. J. Lee, C. S. Chua, L. T. Ong, H. R. Tan, W. R. Webb, R. Raja and Y.-F. Lim, *J. Mater. Chem. A*, 2016, **4**, 9744-9749.